Evaluation of plastic work density, strain energy and slip multiplication intensity at some typical grainboundary triple junctions

Tetsuya Ohashi[1, a], Michihiro Sato[1, b] and Yuhki Shimazu[1, c]

[1]Kitami Institute of Technology, Koencho 165, Kitami, 0908507 Hokkaido, Japan

[a]ohashi@newton.mech.kitami-it.ac.jp, [b]sato@newton.mech.kitami-it.ac.jp, [c]shimayu@newton.mech.kitami-it.ac.jp

Keywords: polycrystals, grainboundary junctions, plastic slip, deformation, dislocations, numerical analysis, finite element analysis, recrystallisation

Abstract. Plastic slip deformations of tricrystals with simplified geometries are numerically analyzed by a FEA-based crystal plasticity code. Accumulation of geometrically necessary (GN) dislocations, distributions of the total slip, plastic work density and GN dislocations on slip systems, as well as some indices for the intensity of slip multiplication are evaluated. Results show that coexistence of GN dislocations on different slip systems is prominent at triple junction of grainboundaries.

Introduction

When polycrystalline metals deform plastically, various kind of inhomogeneous deformation evolve in the microstructure and accumulation of dislocations are observed. Meanwhile, it is generally understood that the microstructure of single phase materials consists of grainboundaries, triple junctions and quadruple points of the boundaries and physically important phenomena are known to take place at or in the vicinity of these structural elements. Among these, grainboundary triple junctions are believed to play a major role in determining the macroscopic mechanical response of polycrystalline materials, nucleation of recrystallisation embryos during thermo-mechanical treatment or generation of crack embryo after some plastic deformation. But quantitative understandings of their roles are not yet obtained.

In this communication, we analyze plastic slip deformation in two models of tricrystals where there is only one grainboundary triple line in each model. The tricrystal models are designed so as that they exhibit wedge- or twist-disclination type deformation field after slip deformation on the primary slip systems in three crystal grains. We employ a crystal plasticity FE code for the numerical analyses where strain hardening and slip multiplications are evaluated by theoretical models for dislocations, while the accumulations of GN dislocations as well as statistically stored (SS) ones are evaluated from the calculated distribution of plastic shear strain on existing slip systems. Distribution of plastic work density, elastic strain energy stored in the model and some measures for the entanglement of dislocations on different slip systems are obtained and discussions are made on generation of embryos of recrystallisation.

Tricrystal models

We employ two tricrystal models, named W-type and T-type models, as shown in Fig. 1. Materials are assumed to be FCC crystals and slip deformations take place on {111}<110> slip systems. Crystal orientations of grain 1, 2 and 3 for two models are the same but the arrangement of crystal grains differs. Slip directions and slip plane normals of the primary slip systems in grains 1, 2 and 3 lie on the x-y plane and the angles between the compression axis and the slip plane normals are 139°, 49° and 41°, respectively. If we denote the increment of plastic shear strain on a slip system n as $\dot{\gamma}^{(n)}$, the plastic strain increment in the specimen coordinate system is given by,

$$\dot{\varepsilon}_{ij}^{p} = \sum_{n} P_{ij}^{(n)} \dot{\gamma}^{(n)} , \tag{1}$$

$$P_{ij}^{(n)} = (b_i^{(n)} n_j^{(n)} + b_j^{(n)} n_i^{(n)})/2 . \tag{2}$$

where, $b_i^{(n)}$, $n_i^{(n)}$ and $P_{ij}^{(n)}$ denote slip direction, slip plane normal and Schmid tensor of the slip system n, respectively. Schmid tensors of the primary slip systems for grains 1-3 are,

$$P_{ij}^{(primary\,system)} = \begin{pmatrix} -0.495 & \mp 0.07 & 0 \\ \mp 0.07 & 0.495 & 0 \\ 0 & 0 & 0 \end{pmatrix}, \tag{3}$$

where, minus sign at the P_{12} components applies to the grain 2, while plus sign applies to grain 1 and 3. If each crystal grain deform individually by slip on the primary system, they exhibit not only the normal strain in x and y-directions but also shear strains ε_{xy} are generated. The magnitude and sign of the shear strain for grains 1 and 3 are the same, but its sign for the grain 2 is opposite to the one in the grain 1 or 3. Therefore, deformation field of wedge and twist disclination types will be formed in the W- and T-type tricrystals, respectively.

We apply a uniformly distributed compressive load on the bottom and top surfaces of the specimens while all the other surfaces are traction free. The initial dislocation density of $1\times10^{12}\,[m^{-2}]$ is given for slip systems and elastic compliance data of isotropic character are used.

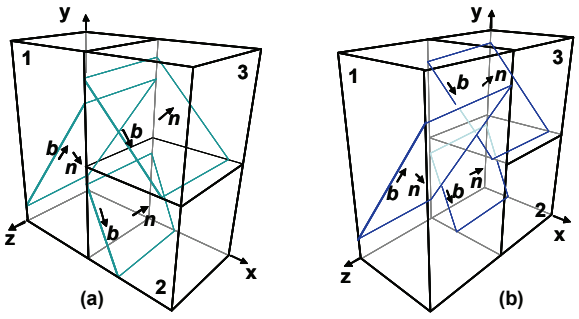

Fig. 1 Tricrystal models of W-type (a) and T-type (b) employed in this study.

Crystal plasticity analysis and GN dislocations

Plastic slip deformation are analyzed by a crystal plasticity software code with the model for the critical resolved shear stress $\theta^{(n)}$ for slip system n, given by [1,2]

$$\theta^{(n)} = \theta_0(T) + \sum_{m=1}^{12} \Omega^{(nm)} a \mu \tilde{b} \sqrt{\rho_S^{(m)}} , \tag{4}$$

where, the first and the second terms in the right hand side are lattice friction and strain hardening terms, respectively. The lattice friction is assumed to be zero in this study. Density of GN dislocations are evaluated by spatial gradient of plastic shear strain by

$$\left\| \rho_G^{(n)} \right\| = \sqrt{(\rho_{G,edge}^{(n)})^2 + (\rho_{G,screw}^{(n)})^2} , \tag{5}$$

$$\rho_{g,edge}^{(n)} = -\frac{1}{\tilde{b}} \frac{\partial \gamma^{(n)}}{\partial \xi^{(n)}} , \quad \rho_{g,screw}^{(n)} = -\frac{1}{\tilde{b}} \frac{\partial \gamma^{(n)}}{\partial \zeta^{(n)}} . \tag{6}$$

We introduce the following quantities,

(7)

$$W^p = \sum_n \int \theta^{(n)} d\gamma^{(n)} , \tag{8}$$

$$\tilde{I}_1 = \sum_n \left\| \rho_G^{(n)} \right\| / \sum_n \rho_{S,0}^{(n)} , \tag{9}$$

$$\tilde{I}_2 = \sum_m \sum_n \omega_2^{(mn)} \left\| \rho_G^{(m)} \right\| \left\| \rho_G^{(n)} \right\| / \sum_m \sum_n \omega_2^{(mn)} \rho_{S,0}^{(m)} \rho_{S,0}^{(n)} , \tag{10}$$

$$\tilde{I}_3 = \sum_k \sum_m \sum_n \omega_3^{(kmn)} \left\| \rho_G^{(k)} \right\| \left\| \rho_G^{(m)} \right\| \left\| \rho_G^{(n)} \right\| / \sum_k \sum_m \sum_n \omega_3^{(kmn)} \rho_{S,0}^{(k)} \rho_{S,0}^{(m)} \rho_{S,0}^{(n)} , \tag{11}$$

where, W^p denotes the plastic work density made by slips on 12 slip systems. $\tilde{I}_1$ is the total of GN dislocations on 12 slip systems divided by the initial value for the grown-in dislocations. When the deformation temperature is relatively high such as in the case for thermo-mechanical treatment, pair annihilation of dislocations with plus and minus sign will result in a rapid decrease of SS dislocations while GN ones will remain since their Burgers vectors are inherently redundant. Thus, $\tilde{I}_1$ is supposed to be a measure for the net density of dislocations after a quick recovery of dislocations at high temperature and the distribution of strain energy stored in the microstructure will be proportional to the one for the $\tilde{I}_1$. $\tilde{I}_2$ and $\tilde{I}_3$ are introduced to evaluate the magnitude of entanglement of dislocations which is supposed to be important also in the process of thermo-mechanical treatment. Inoko [3] introduced a theory for the generation of embryos of recrystallisation where combination of dislocations on two different slip systems were necessary. In his theory, dislocations on two slip systems are supposed to be used to produce a dislocation network and it turns out to be an interface between the embryo and matrix. In a three dimensional case, dislocations on more than three slip systems are necessary to make up a region which is surrounded by entangled dislocation networks and serve as an embryo of recrystallisation. Detailed discussions on the choice of slip systems to produce effective dislocation network for embryo-matrix interface or closed embryo region are not made here, but we assume that $\omega_2^{(mn)} = \omega_3^{(kmn)} = 0$ when the slip systems *n* and *m* share a slip plane or direction, and otherwise $\omega_2^{(mn)} = \omega_3^{(kmn)} = 1$. Thus, $\tilde{I}_2$ is a scale for the magnitude of entanglement of dislocations on two slip systems. There are 48 combinations of two slip systems where their slip planes and Burgers vectors differ. Similarly, $\tilde{I}_3$ gives a scale for the magnitude of entanglement of dislocations on three slip systems. There are 72 combinations of three slip systems where their slip planes and Burgers vectors differ.

Results

Fig. 2 shows distribution of plastic shear strain and work density in the W-type model when the average compressive strain is about 20%. Distribution of plastic shear strain on the primary slip system, $B4:(11\bar{1})[101]$ is not uniform but rather simple, while the distribution of plastic shear strain on a secondary system, $A3:(111)[10\bar{1}]$ is confined to narrow strip regions which originate from the grainboundary triple junction and develop into the interior of the grains 1 and 3. It should be noted that interactions of two crystal grains across a grainboundary plane will not result in this type of activation of slip systems; this kind of interaction will induce multiple slips along grainboundary planes. Activation of A3 system shown in Fig. 2(b) is caused by the interaction of three crystal grains and generation of a deformation field which is analogous to that of wedge type disclinations. Fig. 1(c) shows the distribution of the plastic work density W^p. The plastic work density is not so high at the triple junction but shows higher value at the top and bottom ends of the specimen. It is also understood that contribution from the activity of secondary slip systems to W^p is negligibly small.

Fig. 3(a) and (b) show the density distribution of GN dislocations on the primary and secondary slip systems, respectively. GN dislocations accumulated on these slip systems make up some high density strips inside the grains 1 and 3. Fig. 3(c) depicts the distribution of $\left\| \rho_G^{(B4)} \right\|$ in the T-type

model. Distribution of GN dislocations in the W- and T-type models differ completely.

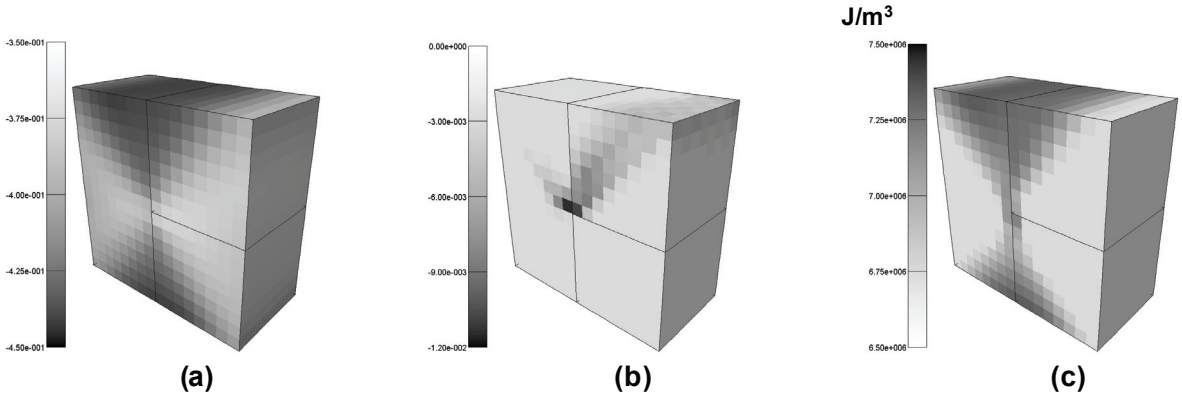

Fig. 2(a) and (b): plastic shear strains on B4 and A3 systems in W-type model, respectively. (c): plastic work density in the W-type model.

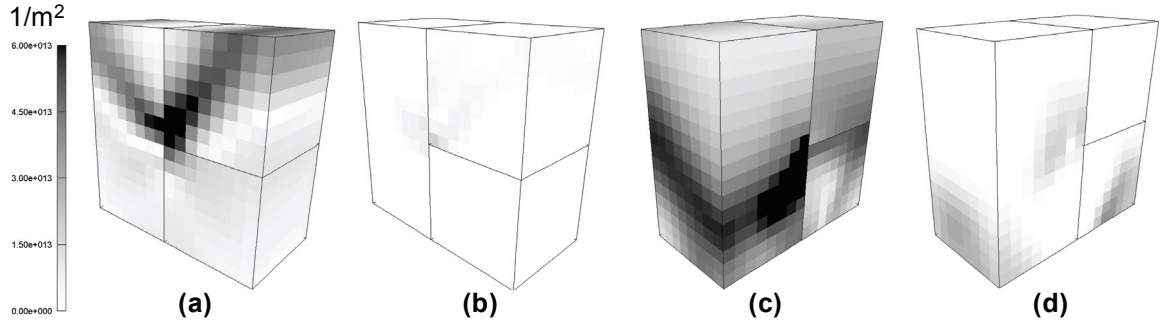

Fig.3 Distributions of the density norm of GN dislocations on B4(a) and A3(b) systems in W-type model, and B4(c) and A3(d) systems in the T-type model.

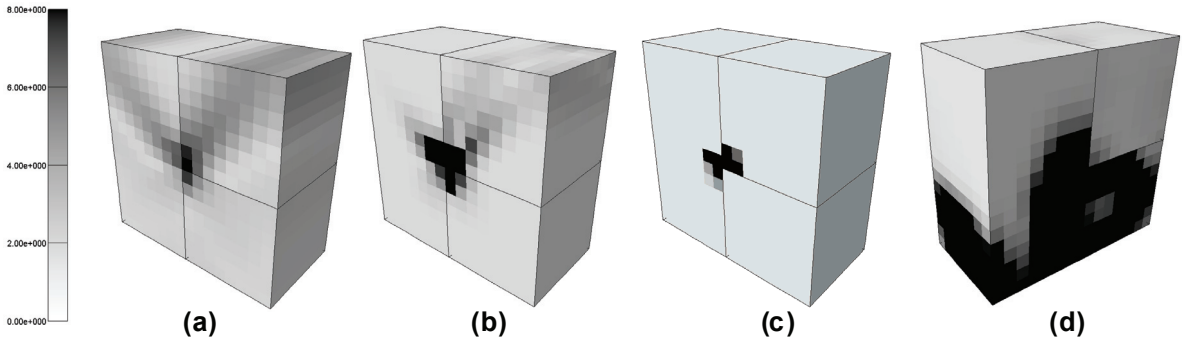

Fig. 4 (a)-(c): Distributions of $\tilde{I}_1$, $\tilde{I}_2$ and $\tilde{I}_3$ in the W-type model. (d) Distribution of $\tilde{I}_2$ in the T-type model.

Figs. 4(a)-(c) show the distribution of $\tilde{I}_1$- $\tilde{I}_3$ in the W-type model. $\tilde{I}_1$ shows the highest value along the triple junction and make up two diffused strip-shaped regions extending into the grains 1 and 3. Distributions of $\tilde{I}_2$ and $\tilde{I}_3$ are more confined near the triple junction. Fig. 4(d) shows the distribution of $\tilde{I}_2$ in the T-type model. Dislocation accumulation and entanglement are more pronounced in the T-type model and their distribution is more complicated.

References

[1] Ohashi, T., Phil. Mag. Lett., vol. 75(1997), 51-57.
[2] Ohashi, T., Int. Journal Plasticity, vol. 21(2005), 2071-2088.
[3] Inoko *et al*., Proc. 4th Int. Conf. Recrsytallization and Related Phenomena, JIM, (1999), 131.